Sensors & Actuators: A. Physical 337 (2022) 113424

Contents lists available at ScienceDirect

Sensors and Actuators: A. Physical

journal homepage: www.journals.elsevier.com/sensors-and-actuators-a-physical

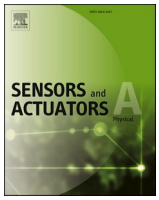

Design and printing of a coplanar capacitive proximity sensor to detect the gap between dielectric foils edges

Rubaiyet Iftekharul Haque, Martin Lubej, Danick Briand *

École Polytechnique Fédérale de Lausanne, Soft Transducers Laboratory, Neuchâtel, Switzerland

ARTICLE INFO

Keywords:
Capacitive
Foil
Gap sensing
Printing
Proximity sensor

ABSTRACT

This paper presents the design and development of a coplanar capacitive proximity sensor for the detection of the gap between the edges of dielectric foils. The finite element analysis is applied to study the design of the sensor by investigating the effects of different physical parameters, like, the sensing electrodes width, the spacing between them and the thickness of the substrate on its responses. The sensitivity of the sensor increases with the ascending electrode width; but is negatively affected by the growing spacing between electrodes. Conversely, the foil edge gap detection range rises with the growing electrode width and spacing between electrodes. Moreover, the optimum sensor performance is observed for the foil edge gap positioned centered with the sensing electrodes and the target foil remaining in contact with its surface. The capacitive proximity sensor with optimum set of parameters is fabricated on a polyimide foil by the inkjet of the sensing electrodes. The sensor demonstrates an average optimum sensitivity of 0.105 fF/μm for an edge gap detection range of 500 μm with a 450 μm thick polyethylene foil, when the vertical gap between the foil and the active area of the sensor is maintained to zero. The sensitivity and the detection range capability reduce significantly with the increasing vertical gap between the sensor and foil.

1. Introduction

Over the past decade, the global packaging industry has experienced steady growth. The trend suggests that the growth will continue for years to come due to economic boom in the emerging markets. In recent time, the plastic packaging is being increasingly used in medical products and healthcare as well as in the beverages and packaged foods due to their low cost, mechanical and thermal properties, and their good barrier characteristics against carbon dioxide, oxygen, and aromatic compounds [1,2].

With the growing implementation of automation, the packaging industries are increasing productivity while maintaining quality at low cost. Monitoring of the processes become of high interest to ensure high production yield. Notably, manufacturing tubular plastic packages, in which precise lamination of the two edges of the foil is required to form the tubes, can suffer from the rotation of the plastic foil within the production machine and from the unwanted movement of the packaging foil edges with respect to the reference during lamination. These can lead to failure in the lamination process and thus causes waste of materials and production time, resulting to an increase of the production cost. For the industries involve in producing seamless tubular plastic, made mainly of polyethylene (PE), it is therefore of high interest to automatize the monitoring and fast detection of the movement of the packing foil edges inside the laminator at high-speed foil motion rate.

Amongst different types of proximity sensors [3], photoelectric sensor [4–6] is commonly used in industries for materials position measurement and monitoring. Although, photoelectric proximity sensors have long detection range and are very reliable, they require costly equipment and high-speed image analysis capability. Moreover, relatively large space is required to mount high speed camera, light source and accessories and might necessitate consequent redesigning of the equipment for mounting the sensor. Capacitive proximity sensor can be an attractive cost-effective alternative to optical sensor [7–11]. The capacitance measurement approach is a low-cost non-destructive technique, that nowadays has been implemented for wide range of applications for examining geometrical and physical parameters [11].

Abbreviations: E_S, Spacing between the electrodes; E_W, Width of the electrodes; F_T, Polyethylene (PE) target foil thickness; G_{FE}, Gap between PE foil edges; M_S, Spacing between grounded metallic guiding rail and sensor holder; P_{FE}, Foil edge gap position with respect to sensor's electrodes center; S_T, Thickness of polyimide (PI) substrate; VG_{SF}, Vertical gap between sensor and target PE foil.

* Corresponding author.
E-mail address: danick.briand@epfl.ch (D. Briand).

https://doi.org/10.1016/j.sna.2022.113424
Received 2 September 2021; Received in revised form 28 January 2022; Accepted 2 February 2022
Available online 8 February 2022

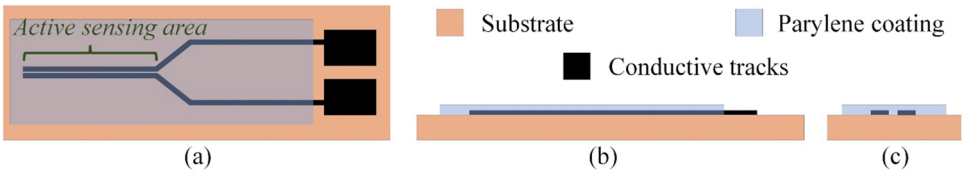

Fig. 1. Schematic diagram of the design of the coplanar capacitive sensor: (a) top view, (b) side on view and (c) front on view.

Capacitive sensors can be fabricated with relative ease, exhibit fast response time, consume low power, and have a lower fundamental noise floor. However, their sensitivity is affected by moisture and temperature. In addition, parasitic capacitance and noise coming from external perturbations can also have an influence on the response of the capacitive sensors, and thus the careful shielding of the system and designing of the reading out electronics is required.

A capacitive proximity sensor consists of pair of electrically conductive electrodes between which a potential difference is applied to generate an electrostatic field. This field is disturbed when a target object is moved close to the sensor and its proximity is detected by the change of capacitance [12,13]. It can detect the presence of any solid body, both metallic and non-metallic objects, since they will affect the capacitance of the sensor relative to the surrounding ground region [14]. To date, capacitive sensors have been employed for various applications, like, assessing aging of composite insulators [15], determining dielectric permittivity and thickness of dielectric plates and shells [9], automobile tire strain measurement [3], force sensing in biomedical applications [16], liquid level detection [8], and yield monitoring in harvest [17]. Different sensor configurations, geometries and designs have been adapted depending on the applications. However, no prior report on the detection of gap between dielectric foil edges using capacitive proximity sensor is available.

Here, we report for the first time on the implementation of a simple capacitive proximity sensor designed for the specific application of detecting the gap between the two edges of a dielectric foil. Using simulation and experimental results, proof of concept has been demonstrated. Amidst different types, the coplanar capacitive sensor configuration has been identified to be the most suited for foil edge gap detection application due to its geometry, non-contact and high sensitivity features. For practical implementation in an industrial tool, the capacitive proximity sensor requires to be thin and flexible. There are several factors influencing the performance of the coplanar capacitive sensor. These include physical parameters of the sensors, namely, the area of the sensing electrodes, the spacing between them, and the thickness of the substrate; as well as external parameters, like, the target foil thickness, rotation of the foil edge with respect to the sensor position, slit gap between grounded metallic guiding rail and sensor holder, and the vertical gap between PE target foil and sensor. The finite element model was developed to study the viability of the design, to understand the effects of different physical and external parameters on the initial capacitance values and responses of the sensor, followed by design optimization. Finally, we demonstrate the realization of the coplanar capacitive proximity sensors using inkjet printing and their characterization.

2. Experimental procedures

2.1. Design and materials

A simple coplanar capacitive design for the sensor is proposed. The sensor design consists of two parallel conductive line electrodes with

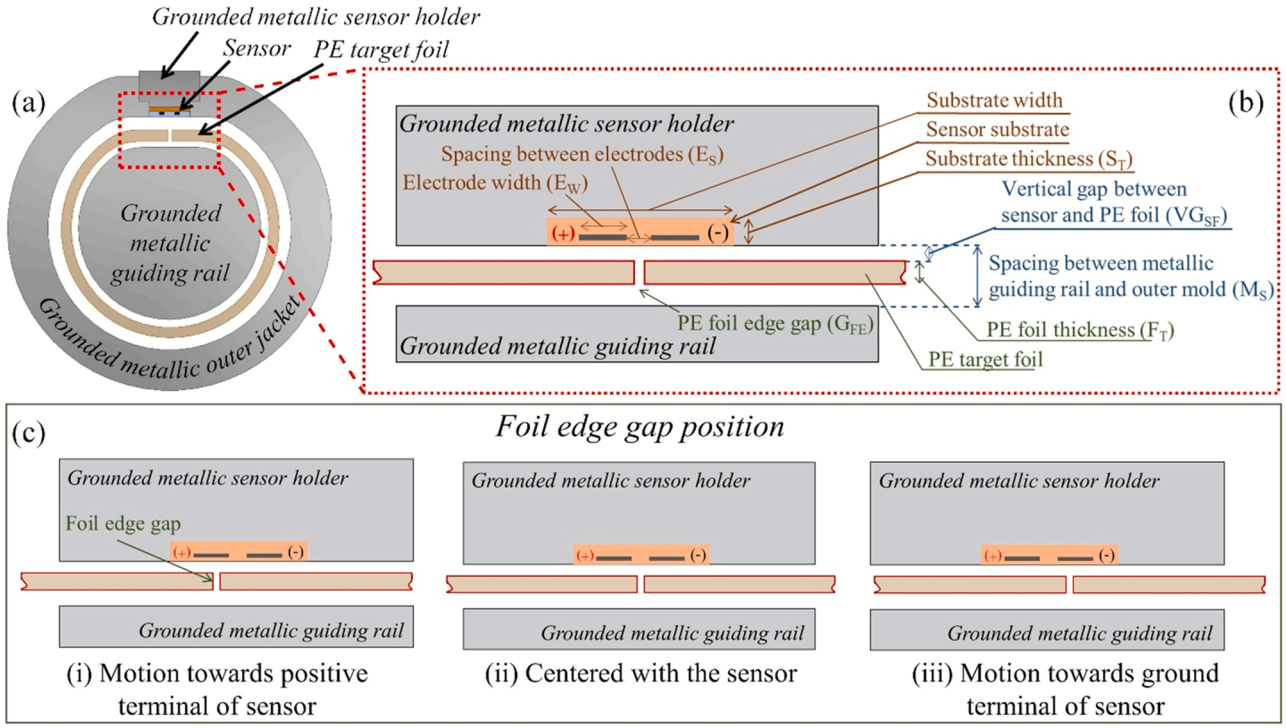

Fig. 2. Schematic diagrams of (a) cross-section view of the tubular packaging process along with sensor mounted on the metallic body of the equipment and PE foil edge position in between metallic parts, (b) cross-section view of the foil edge motion on the coplanar capacitive sensor mounted on the metallic guiding rail and surrounded by metallic sensor holder, and (c) foil edge gap position with respect to the center of the sensing area of the capacitive proximity sensor.

Table 1
List of relative permittivity of the different materials.

Material	Relative permittivity (ε_r)
Polyimide substrate	3.4
Polyethylene foil	2.5
Parylene coating	2.65

narrow spacing between them located on the same plane of the substrate. The electrodes are covered with thin dielectric layer to protect the sensor from wear and tears under friction due to foil motion. The design of the coplanar capacitive sensor is illustrated in Fig. 1. In comparison with a parallel plate capacitor configuration, instead of having to sandwich the target material in between the sensing electrodes, a coplanar capacitive sensor is comprised of separated electrodes that lay in the same plane with the material under test being placed on top of the two electrodes (Fig. 2).

For the coplanar capacitive sensor with identical planar electrodes having length (L) and width (W), the capacitance can be defined by the electrode area (L×W) and center to center spacing between the planar electrodes (s). Since, in general the coplanar sensor is designed with L> >W, and W being kept as a constant value; the electrode area is proportional to L. Therefore, the capacitance (C) of the coplanar capacitor can be expressed as follows [11],

$$C = \frac{\varepsilon_0 \varepsilon_r L}{\pi} ln \frac{(s+W)^2}{s(s+2W)}$$

where ε_0 represents electric constant ($\varepsilon_0 = 8.854 \times 10^{-12}\ Fm^{-1}$) and ε_r represents the relative static permittivity of the dielectric materials.

During the seamless tubular lamination process, the packaging foil, namely, polyethylene (PE), is trimmed according to the required tube circumference. Thereafter, passes through a narrow slit of metallic guiding rail and the sensor metallic holder that folds the foil to create tubular shape by getting foil edges together with ideally no overlap centered with heating unit. The slit between the metallic guiding rail and the sensor holder is adjustable depending on the foil thickness. The edges of the inner layer of the web are, then, edge welded using a hot press lamination process, cooled and cut according to the required length. The regions of the tube forming metallic guide and outer jacket in line with the heating unit where foil edges meet is leveled to perform hot press. In a closed-loop manufacturing operation, an inspection of the position of the foil edges would need to be performed just before the welding segment, where a tiny removable metallic window block of the outer jacket is located for adjusting the placement of the foil edges prior to lamination. The sensor should have a small footprint in terms of area, and thickness within several hundred microns due to the availability of limited space within the metallic guides to mount the sensor. Metallic parts are grounded to minimize noise. Fig. 2(a) illustrates the simplified cross-section view of the process to detect the gap between foil edges, where the sensor is mounted on the small removable metallic holder having flat surface, and the dielectric foil passes over the sensor guided by the slit created by the holder and the guiding rail.

The silver nanoparticle-based ink (Suntronic Jet Silver U5603) from Sun Chemical was employed to print the electrodes. The polyimide (PI) foil from Sichuan Coxin Insulating Material Co., Ltd., Deyang City, Scihuan, China, and the microscope glass slides from Thermo Scientific, have been used as substrate to develop the flexible and the rigid sensor, respectively. A Parylene insulating film was applied as protective coating on the sensor element.

2.2. Simulations

Based on the configuration shown in Fig. 2(b), a finite element method (FEM) model of the coplanar capacitive proximity sensor is developed that incorporates the effect of the grounded metallic surroundings. The numerical analysis enables us not only to study the responses of the sensor for varying foil edge gap size and position, but also to investigate and to quantify the effects of different physical and external parameters on these responses. Numerical simulation was performed employing COMSOL Multiphysics software (version 5.3a). The custom mesh is used for efficient resolving of the model geometry. Table 1 provides the list of relative permittivity of substrate material, target PE foil material and protective coating layer used during numerical analysis.

Table 2
List of experimental variables and their ranges use for numerical analysis.

Parameter	Range value
PE target foil thickness (F_T)	200 & 450 μm
Thickness of PI substrate (S_T)	40 – 200 μm
Width of the electrodes (E_W)	100 – 400 μm
Spacing between the electrodes (E_S)	10 – 200 μm
Vertical gap between sensor and target PE foil (VG_{SF})	0 – 300 μm
Foil edge gap position with respect to sensor's electrodes center (P_{FE})	-500 – 500 μm
Spacing between grounded metallic guiding rail and sensor holder (M_S)	300 – 500 μm

Two different target foil thicknesses of 200 μm and 450 μm are considered, corresponding to the two most commonly used PE foil thickness by the industry to produce seamless tubular plastic packages. Initial study and tests reveal that the dielectric properties and performance of the coplanar capacitive proximity sensor are linked with several dimensional parameters of the sensor. For example, length and width of the sensing electrodes and the spacing between them, the substrate thickness, and the presence of a protective layer coating, have affected the responses of the sensors. During the study, the length of the electrodes and the protective coating layer thickness were kept constant to 10 mm and 2 μm, respectively. In addition, some external factors, like the spacing between the grounded metallic guiding rail and sensor holder through which the PE foil slides, and the vertical gap between sensor and target foil (VG_{SF}), which refers to whether the target foil is in physical contact with the active area of sensor or not, and the position of the gap between the edges of the foil with respect to the electrodes of the sensor, are contributing to the characteristic of the sensor. The ranges of the input parameters used in the numerical experiments are presented in Table 2. These values were selected based on the constrains of the industrial lamination equipment and our sensor fabrication process capabilities.

A series of FEM analysis are performed to investigate and eventually to optimize the sensor to fulfill the requirements for the detection of the varying gap between the PE foil edges (G_{FE}). The absolute capacitance (C_0), sensitivity ($\Delta C/\Delta G_{FE}$) that attributes the capacitance variation (ΔC) due to changing foil edge gap, the relative capacitance variation ($\Delta C/C_0$) and the gap detection range of the sensor, referring to the maximum detectable PE edges gap can be sensed by the sensor, are analyzed for each study. Initially, the classic one-variable-at-a-time approach is adopted, where the effect of individual input factor on the response of the sensor is examined for a fixed set of other input parameters. The process is repeated for each of the input parameters involved in the study. Finally, the optimization interface in COMSOL involving the 'Sparse Nonlinear OPTimizer (SNOPT)' solver method is employed to obtain the set of optimal parameters for the coplanar capacitive proximity sensor to achieve maximized sensitivity and edge gap detection range of at least 250 μm. In this regard, only major influential input parameters are varied simultaneously while keeping other factors fixed and set criteria is used to achieve the optimum set of parameters for the sensor that fulfill the benchmark.

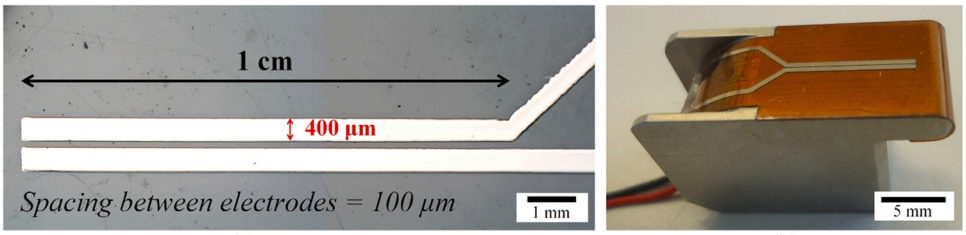

Fig. 3. (a) Optical image of the inject printed coplanar capacitive proximity sensor on glass substrate (top view), and (b) photograph of the flexible proximity sensor printed on PI substrate mounted on metallic holder.

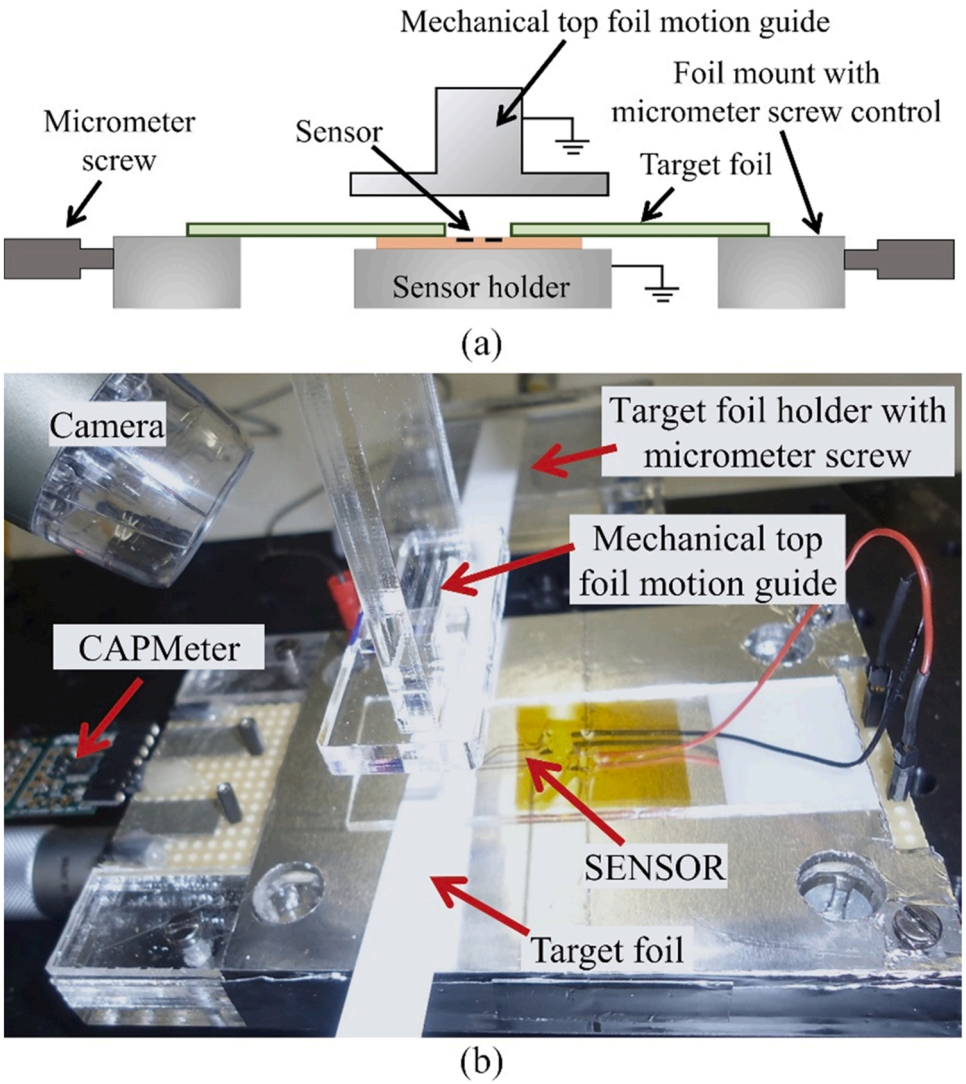

Fig. 4. (a) Schematic diagram of the experimental setup, and (b) photograph of the experimental setup to measure the capacitance variation with respect to gap between the foil edges.

2.3. Fabrication

Inkjet printing technique was favored for the sensors fabrication as it is contact free, it allows customized pattern design by its digital nature, and is well adapted for patterning thin films on flexible foils [7,18–22]. The coplanar capacitive proximity sensors were fabricated by a drop-on-demand (DoD) piezoelectric Dimatix 2800-DMP inkjet printer from Fujifilm using 10 pL cartridges that consists of 16 nozzles. During printing, the nozzle temperature of 32 °C and the plate temperature of 28 °C is used. Sensors were produced, with optimized set of dimensional parameters, using silver ink on rigid microscope glass slides with a thickness of 1 mm, and its flexible final version on polyimide foils having a thickness of 75 µm. These two different substrates in terms of materials and thickness were used to verify the model.

First, the substrate is cleaned using isopropanol (IPA), dried and followed by oxygen plasma treatment. Then the transducing electrodes are patterned by inkjet-printing of the silver nanoparticle ink with the drop spacing of 20 µm. Thereafter, ink curing is performed at 140 °C for

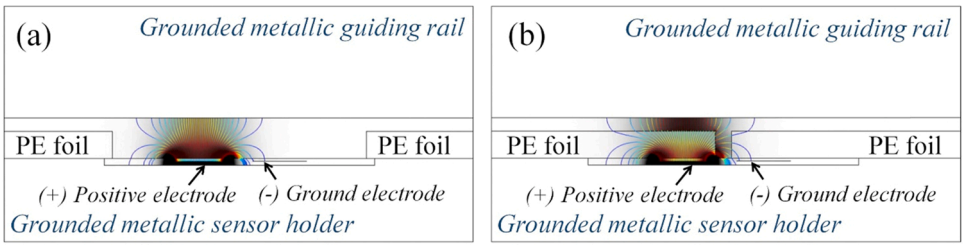

Fig. 5. Change of electrostatic field of the coplanar capacitive proximity sensor due to sliding of the dielectric PE foil edges overlapping the active area of the sensor from finite element analysis.

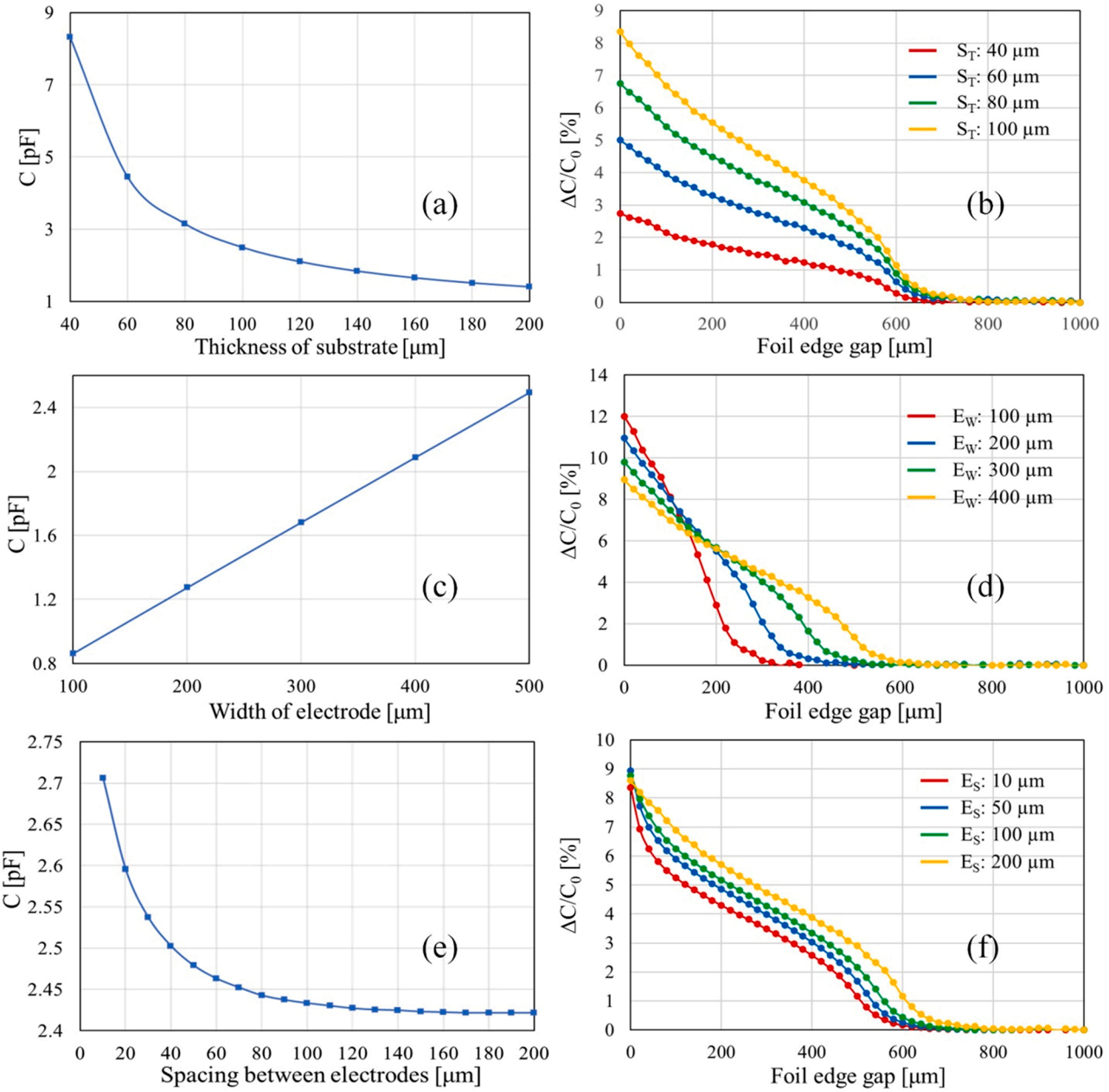

Fig. 6. Numerical analysis to study the effects of physical parameters of the coplanar capacitive proximity sensor on its absolute capacitance and its response to foil edge gap variations for varying (a, b) thickness of the substrate (S_T) for fixed $E_W = 400$ µm, $E_S = 50$ µm, (c, d) width of the electrode (E_W) for constant $S_T = 100$ µm, $E_S = 50$ µm, and (e, f) spacing between electrodes (E_S) while maintaining $S_T = 100$ µm, $E_W = 400$ µm, while keeping $M_S = 300$ µm, $F_T = 200$ µm, $VG_{SF} = 0$ µm & P_{FE} centered with sensor.

30 min in thermal oven. The 2 μm thick Parylene C coating is deposited using Comelec C-30-S reactor at room temperature. Fig. 3 illustrates microscopic image of the inkjet-printed proximity sensor and the photograph of the flexible sensor mounted on the metallic part of the industrial equipment.

2.4. Characterization

The dimensions and the microstructures of the printed conductive layers were studied using optical digital microscope (HIROX model: KH-8700) and optical profiling system (WYKO NT1100 from Veeco). The static capacitance of the device and its variation with the package foil over it was measured using a CAPMeter having 24 bits DAC converter with 2 channels and range of ± 4 pF with resolution down to 4 aF from JLM Innovation, Germany, with 10 ms data acquisition interval setting. A custom-made test setup to measure the capacitance variation with respect to target PE foil edge gap was developed as presented in Fig. 4. The test bench consists of micrometer screw to control the spacing between the foil edges. The setup allowed us to recreate and maintain the gap between the grounded metallic parts through which the target PE foil edges can move.

3. Results and discussion

3.1. Numerical analysis and design optimization

The capacitive proximity sensor works by detecting the modulation of active electrostatic field due to approaching dielectric or metallic object within the field and thus encounter the change of capacitance. When the dielectric object approaches, either horizontally or vertically, towards the coplanar capacitive sensor, the change of electrostatic field occurs due to change of effective dielectric permittivity. Thus, the capacitance of the sensor changes. As illustrated with finite element in Fig. 5, change of electrostatic field is observed due to lateral sliding of the edges of target PE dielectric foil, having higher dielectric permittivity than air, towards the sensor from outside to cover the sensing region.

3.1.1. Sensors design parameters

The numerical analysis is first performed to understand the influence of different physical parameters of the flexible coplanar capacitive proximity sensor, such as the width of the electrodes (E_W), the spacing between the electrodes (E_S), and the thickness of substrate (S_T). During the process, other factors are kept constant with the spacing between grounded metallic guiding rail and sensor holder (M_S) = 300 μm, the PE target foil thickness (F_T) = 200 μm, the vertical gap between sensor and target PE foil (VG_{SF}) = 0 μm, and the foil edge gap position centered with respect to the center of the sensing region of the sensor (P_{FE}). The effects of varying thickness of the substrate for fixed electrodes dimensions, E_W = 400 μm and E_S = 50 μm, of modifying the width of the electrode for constant substrate thickness and electrodes spacing, S_T = 100 μm and E_S = 50 μm, and of changing the spacing between electrodes while maintaining S_T = 100 μm and E_W = 400 μm constant, are shown in Fig. 6(a-f). The absolute capacitance and responses of the coplanar capacitive proximity sensor for the detection of the varying gap between the PE foil edges for the aforementioned conditions are presented.

The absolute capacitance of the sensor is strongly influenced by the thickness of the substrate, as presented in Fig. 6(a). The thinner substrate contributes to the higher absolute capacitance value of the sensor and strongly decayed with the increasing substrate thickness. For example, the capacitance value drops exponentially from 8.3 pF to 1.4 pF for the change of substrate thickness from 40 μm to 200 μm. The absolute capacitance of the sensor, however, increases linearly with the increasing electrode width (Fig. 6(c)). An increase by about 190% of the absolute capacitance value is recorded for the electrode width going from 100 μm to 400 μm. Furthermore, a smaller spacing between the electrodes leads to the higher absolute capacitance value, which decreases exponentially with the increasing spacing between the electrodes (Fig. 6(e)). The absolute capacitance drops by 10.4% by making larger the spacing between the electrodes from 10 μm to 200 μm. Thus, amongst the dimensional parameters, spacing between the electrodes has much less influence compared to the electrode width on the absolute capacitance of the sensor.

Table 3
Set of optimized physical parameters for the coplanar proximity sensor.

Optimum parameter	Value
Length of electrode (E_L)	10 mm
Width of electrode (E_W)	400 μm
Spacing between electrodes (E_S)	100 μm

In terms of the detection of the gap between the foil edges, the response, sensitivity, and the relative capacitance variation ($\Delta C/C_0$) of the capacitive sensor were computed as a function of the gap range. The width of the electrodes and spacing between the electrodes are the major input factors that influence the response of the proximity sensor. The substrate thickness shows little effect on the sensitivity and the gap detection range; however, strongly influences the relative capacitance variation ($\Delta C/C_0$), as shown in Fig. 6(b). For the low thickness of the substrate, the $\Delta C/C_0$ response is low and increases with the rising substrate thickness. The sensitivity is moderately influenced by the width of the electrode but significantly affects the gap detection range (Fig. 6(d)). The wider electrode contributes to larger gap detection range, however, provides lower sensitivity and thus the $\Delta C/C_0$. The foil edge gap detection range increases from 300 μm to 600 μm, whereas the sensitivity decreased by ~21.8%, for the sensor with electrode width of 100 μm and 400 μm, respectively. Finally, as Fig. 6(f) illustrates, the effect of the spacing between electrodes is low on the sensitivity and gap detection range of the sensor. Small spacing between electrodes contributes to slightly higher sensitivity, whereas wider spacing between electrodes contributes to slightly higher edge gap detection range. The sensitivity drops by 5.1%, whereas the edge gad detection range increase by ~20% for the growing spacing between electrodes from 10 μm to 200 μm. Therefore, to maximize the sensitivity of the sensor, the width of the electrodes and the spacing between them need to be calibrated to minimize noise issue during detection.

Following the understanding of the effects of the individual physical parameters on the response of the sensor, its design parameters were adjusted to optimize both the sensitivity of the sensor and the foil edge gap detection range. During this process, the width of the electrode and the spacing between electrodes are varied together, since these are the two major factors that influence the sensitivity and foil edge gap detection range of the sensor. Other parameters were kept constant with S_T = 100 μm, M_S = 300 μm, F_T = 200 μm, VG_{SF} = 0 μm and P_{FE} centered with sensor. The estimated set of optimum physical parameters for the coplanar capacitive proximity sensor is listed in Table 3. The sensor with the optimum parameters provides a gap detection range of 500 μm, exhibiting the sensitivity of 0.5 fF/μm for the target foil thickness of 200 μm.

3.1.2. Effect of external factors

Numerical analysis also demonstrated that the performances of the coplanar capacitive proximity sensor are affected by several external factors. The effects of target PE foil thickness, position of the foil edge gap with respect to the center of the active sensing region of the sensor, spacing between grounded metallic guiding rail and sensor holder, and finally the vertical gap between the sensor and the target PE foil, on the performances of the proximity sensor are presented in Fig. 7. The optimum sensors design parameters from Table 3 were applied for a fixed substrate thickness (S_T) of 100 μm, since the substrate thickness having

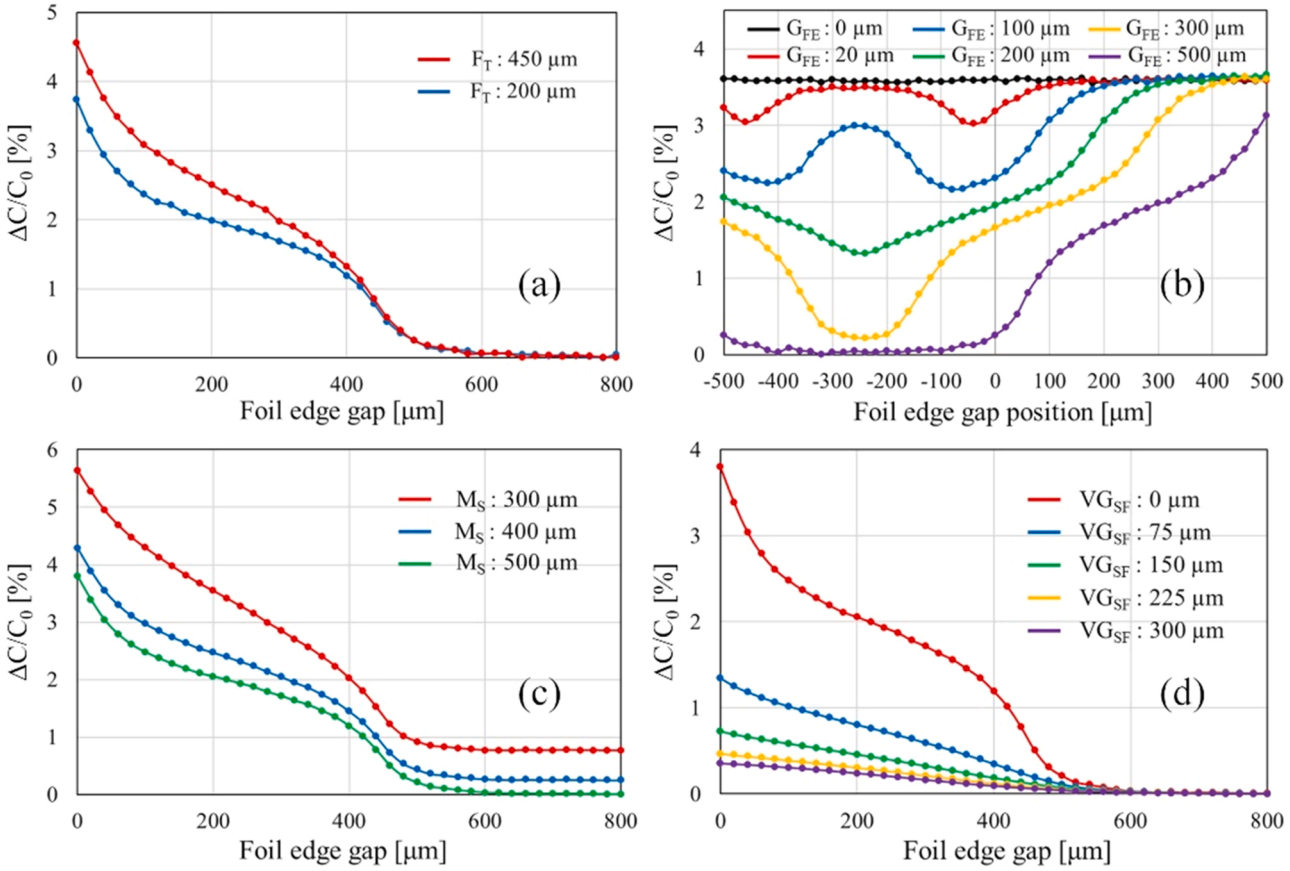

Fig. 7. Numerical analysis to study the effects of varying external factors on the relative capacitance variations of the coplanar capacitive proximity sensor, with a substrate thickness $S_T = 100$ µm, for varying (a) PE target foil thickness (F_T) while keeping $M_S = 500$ µm, $VG_{SF} = 0$ µm and P_{FE} centered with sensor fixed, (b) position of the foil edge gap with respect to the center of the sensor for $M_S = 500$ µm, $F_T = 200$ µm and $VG_{SF} = 0$ µm, (c) spacing between grounded metallic guiding rail and sensor holder (M_S) for constant $F_T = 200$ µm, $VG_{SF} = 0$ µm and P_{FE} centered with sensor, and (d) vertical gap between the sensor and the target PE foil (VG_{SF}) for fixed $M_S = 500$ µm, $F_T = 200$ µm, $VG_{SF} = 0$ µm and P_{FE} centered with sensor, on the responses of the coplanar capacitive proximity sensor while foil edge gap (G_{FE}) detection. Sensors design parameters are summarized in Table 3.

mainly an influence on the capacitance value of the sensor. In this process amongst external factors, when varying one of them, the others were kept constant at the target PE foil thickness (F_T) = 200 µm, the position of the foil edge gap with respect to the center of the sensing region of the sensor (P_{FE}) being centered, the spacing between grounded metallic guiding rail and sensor holder (M_S) = 500 µm, and the vertical gap between the sensor and the target PE foil (VG_{SF}) = 0 µm.

Fig. 7(a) illustrates the effect of target PE foil thickness of 200 µm and 450 µm on the response of the proximity sensor, for $M_S = 500$ µm, $VG_{SF} = 0$ µm and P_{FE} being centered with the sensor. The PE thickness does not have an influence on the foil edge gap detection range, which remains constant at 500 µm, while as expected a higher sensitivity and the relative capacitance variation is recorded for the thicker target foil, at 0.245 fF/µm for $F_T = 450$ µm in comparison to 0.14 fF/µm for $F_T = 200$ µm. The thick target foil replaces thicker layer of air between the grounded metallic slit with a higher dielectric constant material explaining this enhanced sensitivity. During the lamination process, the foil occasionally tends to rotate along the metallic guiding rail and thus drives the foil edge gap position off center, as illustrated in Fig. 2(c). The effect of varying position of the foil edge gap from − 500–500 µm with respect to the center of sensing region on the responses of the sensor for $M_S = 500$ µm, $F_T = 200$ µm and $VG_{SF} = 0$ µm is shown in Fig. 7(b). The negative and positive signs in graph, respectively, refer to the rotation of edge gap towards positive terminal and ground of the sensor. For the foil edge gap of 0 µm, electrodes are fully covered by the foil and thus the position of the foil edge gap (P_{FE}) toward positive or ground terminal exhibits similar signal with little fluctuation. However, distinguishable responses are observed depending on the position of the foil edge gap towards positive or ground terminal when foil edge gap (G_{FE}) is opened. The capacitance increases when G_{FE} moves towards the ground terminal, since positive terminal gets covered by the foil and higher percentage of electrostatic field lines passes through the foil. While G_{FE} moves towards the positive terminal of the sensor, capacitance decreases as the electrostatic field lines go across the air until the gap pass over the terminal fully. Larger the foil edge gap, bigger drops in capacitance are observed for the P_{FE} towards the positive terminal. The best responses from the sensor were recorded for the edge gap position centered with respect the sensing region of the sensor. For practical application, multiple sensing electrodes beside present central sensor electrodes can be introduced and by comparing their responses in situ centered position of the target foil edge gap can be ensured.

In addition, the change of the spacing between the grounded metallic guiding rail and the sensor holder (M_S), that is required to adjust depending on the PE target foil thickness, affects the electrostatic field of the capacitive sensor. The change of M_S from 500 µm to 300 µm, for a constant foil thickness, F_T, of 200 µm, with $VG_{SF} = 0$ µm and P_{FE} being centered with the sensor, led to the increase of base capacitance by ~0.8% (Fig. 7(c)). The sensitivity of the sensor increases by 98.3% with the decrease of the spacing M_S from 500 µm to 300 µm, while the foil edge gap detection range remains again unchanged at 500 µm. Furthermore, the sensitivity and the $\Delta C/C_0$ of the sensor reduced sharply with the increasing vertical gap between sensor and target PE foil (VG_{SF}), while other factors were kept constant at $M_S = 500$ µm, $F_T = 200$ µm, and P_{FE} still being centered with the sensor. For the spacing

Table 4
Parameters of the printed sensors.

Physical parameters		Values
Length of electrode	:	10 mm
Width of electrode	:	400 ± 10 μm
Thickness of the electrode	:	500 ± 50 nm
Spacing between electrodes	:	100 ± 2.5 μm
Parylene layer thickness	:	2 μm

M_S of 500 μm and foil thickness F_T of 200 μm, the vertical gap VG_{SF} can be varied between 0 μm and 300 μm, as shown in Fig. 7(d). The sensitivity for the edge gap detection drops about exponentially by ~77.8% due to increasing VG_{SF} from 0 to 300 μm. The sensitivity of 0.159, 0.062 and 0.035 fF/μm for the VG_{SF} of 0, 150 and 300 μm are observed, respectively. Therefore, to obtain best performance for the foil edge gap detection, the vertical gap between the sensor and the target PE foil (VG_{SF}) needs to be minimum, ideally both being in contact.

Hence, depending on the target foil thickness used during the lamination process, the spacing between the grounded metallic guiding rail and the sensor holder requires to be adjusted in a way that vertically the foil edge remains in close proximity or in contact to the sensor to maximize the sensitivity of the sensor, and thus to improve signal-to-noise ratio.

3.2. Experimental results

Coplanar capacitive sensors with the optimum set of design parameters based on the numerical simulation, as aforementioned (see Table 3), were printed using inkjet printing method on both glass and flexible PI substrates, as shown in Fig. 3. The physical dimensions of the printed flexible sensor were measured and listed in Table 4.

Initially, the sensor was printed on the rigid substrate and compared with the FEM model. In this regard, the sensor printed on glass substrate was used in combination with a 450 μm thick PE target foil. The vertical gap between the sensor and the target PE foil was maintained to the minimum using the setup showed in Fig. 4. The numerical analysis and experimental results of this sensor configuration on glass substrate for the edge gap detection is shown in Fig. 8(a, b). As the results indicate, the capacitance value drops exponentially with the increasing foil edge gap as observed for the numerical simulations. The capacitance decreases from 0.88 pF for a foil edge gap of ~0 μm to 0.828 pF for a foil edge gap of 1 mm, with the drop of relative capacitance variation by 6.35%. The experimental results are in good agreement with the numerical analysis with little fluctuation at high foil edge gap. In addition, a slight deviation is observed at zero edge gap position, that arises due to not being able to achieve total zero edge gap experimentally. These results validate the numerical model.

The coplanar capacitive sensor, printed on PI substrate coated with the Parylene layer, is very thin, flexible, and thus can be easily mounted on the metallic holder as shown in Fig. 3(b). The fabricated flexible sensor exhibits the absolute capacitance of 1.354 pF. The experimental performance of the coplanar capacitive proximity sensors while detecting the gap between the edges of the PE foil is presented in Fig. 8 (c, d). The sensor exhibits, for the PE target foil thickness of 450 μm, the average sensitivity of 0.105 fF/μm of gap, and a gap detection range of 500 μm. The hysteresis characteristics of sensors was also evaluated. The responses of the sensor while opening and closing gap between the foil

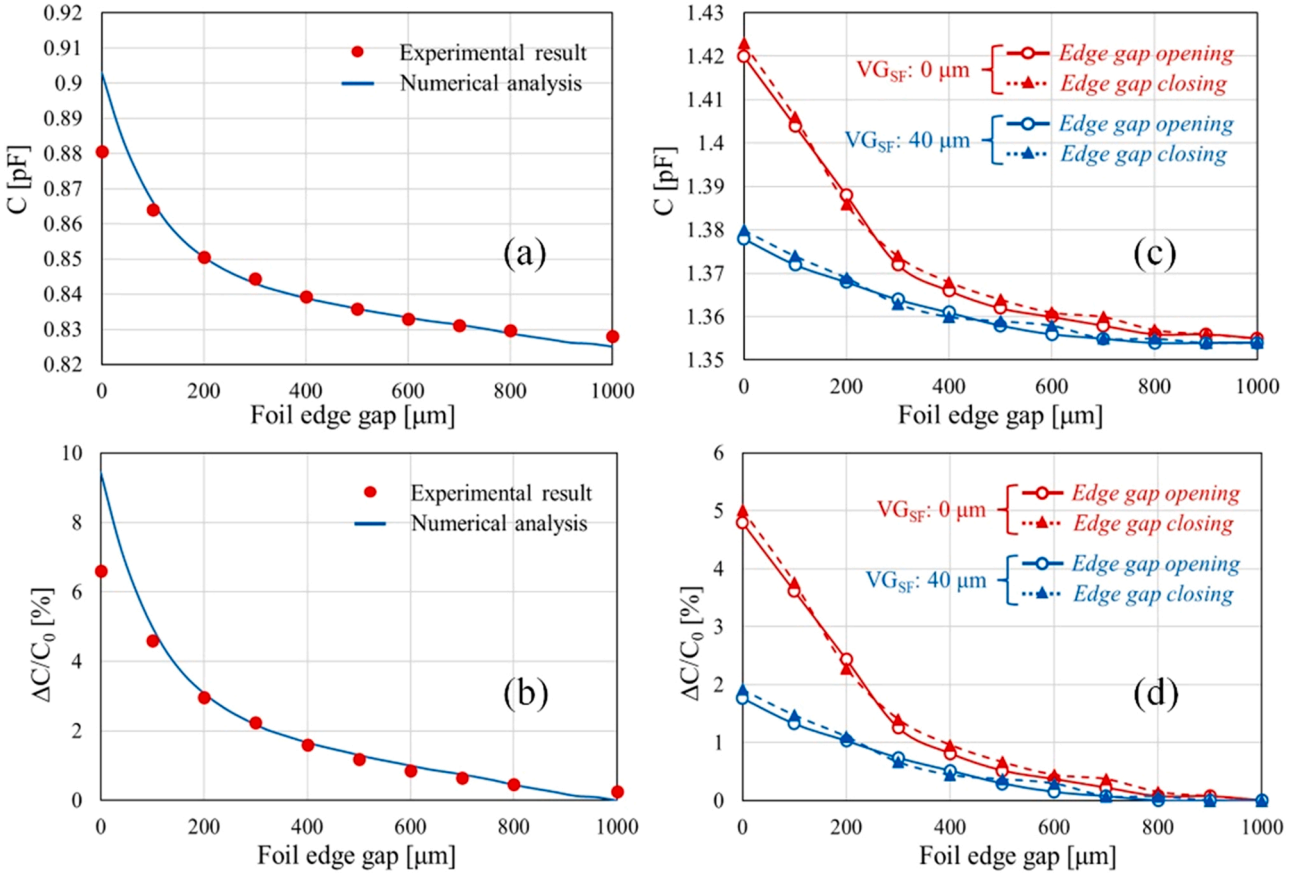

Fig. 8. Responses of the printed coplanar capacitive sensor having optimum parameters while varying target PE foil edge gap: (a, b) comparison between experimental result and numerical analysis of the sensor printed on glass substrate while the vertical gap between the sensor and the foil (VG_{SF}) maintained constant to zero, and (c, d) experimental responses and hysteresis characteristic of the flexible proximity sensors printed on PI substrate for VG_{SF} of 0 μm and 40 μm (solid line refers to foil edge gap opening and dotted line refers to the edge gap closing).

edges are presented with solid and doted lines, respectively, in Fig. 8(c, d). The proximity sensors during foil edge gap opening and closing provided repeatable responses with very little fluctuation and minimum hysteresis. As expected, the significant reduction of the sensitivity and the relative capacitance variations of the coplanar capacitive sensor was observed with the increasing vertical gap between sensor and target foil. The average sensitivity drops by ~63.8% already, to 0.038 fF/μm for a gap detection range of 500 μm, while a vertical gap between the sensor and the PE foil is 40 μm. This result indicates that attention should be paid to have the foil in contact with the sensor for reliable and more sensitive measurements.

4. Conclusion

We have developed a simple coplanar proximity sensor configuration with two parallel electrodes for the detection of the gap between the edges of a polymeric. A FEM model was applied to understand the effects of individual physical parameters to optimize the sensor design and to study the characteristics of the sensor under different circumstances. The grounding of the metallic rail and outer jacket in the model influence the sensor performance due to coupling effect and provide slightly higher sensitivity. Amongst the dimensional parameters, the width of the electrodes and the spacing between them has a higher influence on the sensitivity, whereas the edge gap detection range was mainly affected by the electrode width and moderately affected by the spacing between the electrodes. Furthermore, the enhanced performance of the sensor was reported for the foil edge gap positioned centered with the sensing area, while the target foil remains in close proximity to the surface of the sensor. The sensor with an optimum configuration was fabricated employing inkjet printing technique on thin polyimide substrate. Experimentally for the flexible proximity sensor, the foil edge gap measuring range of 500 μm with the average sensitivity of 0.105 fF/μm has observed for a polyethylene target foil having a typical thickness of 450 μm. With this sensor configuration, a precision of ~40 μm could be reached in the edge gap detection for the considered polyethylene foil. The next step is to integrate multiple sensing electrodes in a sensor, since this might enhance the foil edge gap detection range and will allow quick definitive recognition of both directional rotation of the gap between foil edges with respect to center by in situ comparison of responses of multiple sensors.

CRediT authorship contribution statement

All persons who meet authorship criteria are listed as authors, and all authors certify that they have participated sufficiently in the work to take public responsibility for the content, including participation in the concept development, methodology, design, analysis, fabrication, writing, or revision of the manuscript.

Declaration of Competing Interest

The authors declare that they have no known competing financial interests or personal relationships that could have appeared to influence the work reported in this paper.

Acknowledgements

The authors would like to acknowledge AISA Automation Industrielle SA, Vouvry, Switzerland for the partial funding of the project. We acknowledge also the equipment funding from SNF Project 206021:164028 “Aerosol Jet Tool for Additive Manufacturing and 3D Printing for Microsystems”.

References

[1] S.T. Sam, M.A. Nuradibah, K.M. Chin, Nurul Hani, Current Application and Challenges on Packaging Industry Based on Natural Polymer Blending Natural Polymers ed Ololade Olatunji, Springer International Publishing, Cham, 2016, pp. 163–184.
[2] Nitaigour Mahalik, Advances in packaging, Methods, Process. Syst. Chall. 5 (2014) 374–389.
[3] Zhang Peng, Sensors and Actuators for Industrial Control Industrial Control Technology ed Peng Zhang, William Andrew, NY, USA, 2008, pp. 1–186.
[4] Ondrej Pribula, Michal Janošek, Jan Fischer, Optical position sensor based on digital image processing, Magn. Field Mapp. Improv. Radio. 20 (2011) 6.
[5] V. Osadcuks, A. Pecka, A. Lojans, A. Kakitis, Experimental research of proximity sensors for application, Agron. Res. (2014) 955–966.
[6] R. Aasin Rukshna, S. Anusha, E. Bhuvaneswarri, T. Devashena, Interfacing of proximity sensor with My-RIO toolkit using LabVIEW, Int. J. Sci. Res. Dev. 3 (2015) 5.
[7] Qiang Yang, Andrew J. Yu, James Simonton, Gaoqiang Yang, Yeshi Dohrmann, Zhenye Kang, Yifan Li, Jingke Mo, Feng-Yuan Zhang, An inkjet-printed capacitive sensor for water level or quality monitoring: investigated theoretically and experimentally, J. Mater. Chem. A 5 (2017) 17841–17847.
[8] Daniel Paczesny, Grzegorz Tarapata, Marzęcki Michał, Ryszard Jachowicz, The capacitive sensor for liquid level measurement made with ink-jet printing technology, Procedia Eng. 120 (2015) 731–735.
[9] Matiss Imants, Multi-element capacitive sensor for non-destructive measurement of the dielectric permittivity and thickness of dielectric plates and shells, NDTE Int. 66 (2014) 99–105.
[10] Edin Terzic, Jenny Terzic, Romesh Nagarajah, Muhammad Alamgir, Capacitive sensing technology. A Neural Network Approach to Fluid Quantity Measurement in Dynamic Environments, Springer London, London, 2012, pp. 11–37.
[11] Baxter Larry K, in: Robert J. Herrick (Ed.), Electrostatics Capacitive Sensors: Design and Applications Ieee Press Series on Electronics Technology, IEEE Press, New York, 1997, pp. 6–36.
[12] Bolton William, Instrumentation System Elements Instrumentation and Control Systemns, Newnes, Tokyo, 2015, pp. 15–65.
[13] Andreas Braun, Reiner Wichert, Arjan Kuijper, Dieter W. Fellner, Capacitive proximity sensing in smart environments, J. Ambient Intell. Smart Environ. 7 (2015) 483–510.
[14] Bates Martin, Input Sensor Interfacing PIC Microcontrollers, Newnes, Tokyo, 2014, pp. 299–332.
[15] Jingpin Jiao, Liang Li, Bin Wu, Cunfu He, Novel capacitive proximity sensors for assessing the aging of composite insulators, Sens. Actuators A Phys. 253 (2017) 75–84.
[16] Andrea Bodini, Stefano Pandini, Emilio Sardini, Mauro Serpelloni 2018 Design and fabrication of a flexible capacitive coplanar force sensor for biomedical applications 2018 IEEE Sensors Applications Symposium (SAS) 2018 IEEE Sensors Applications Symposium (SAS) (Seoul, Korea (South): IEEE) pp 1–5.
[17] Chiho Kim, Mankwon Choi, Taejong Park, Myeongil Kim, Kwangwook Seo, Hyeontae Kim, Optimization of yield monitoring in harvest using a capacitive proximity sensor, Eng. Agric. Environ. Food 9 (2016) 151–157.
[18] S. Kholghi Eshkalak, A. Chinnappan, W.A.D.M. Jayathilaka, M. Khatibzadeh, E. Kowsari, S. Ramakrishna, A review on inkjet printing of CNT composites for smart applications, Appl. Mater. Today 9 (2017) 372–386.
[19] N.C. Raut, K. Al-Shamery, Inkjet printing metals on flexible materials for plastic and paper electronics, J. Mater. Chem. C 6 (2018) 1618–1641.
[20] Rubaiyet Haque, R.émy Vié, Michel Germainy, Laurie Valbin, Patrick Benaben, Xavier Boddaert, Inkjet printing of high molecular weight PVDF-TrFE for flexible electronics, Flex. Print. Electron. 1 (2016), 015001.
[21] Lo Li-Wei, Shi Hongyang, Wan Haochuan, Xu Zhihao, Tan Xiaobo, Wang Chuan, Inkjet-printed soft resistive pressure sensor patch for wearable electronics applications, Adv. Mater. Technol. 5 (2020), 1900717.
[22] Sawyer B. Fuller, Eric J. Wilhelm, Joseph M. Jacobson, Ink-jet printed nanoparticle microelectromechanical systems, J. Micro Syst. 11 (2002) 54–60.

Rubaiyet I. Haque received his Ph. D. in microelectronics from the École Nationale Supérieure des Mines de Saint-Étienne, France in 2015. He obtained B.Sc. (Hons.) in Physics from Chittagong University, Bangladesh, and carried out ‘Joint European Masters in Materials Science’. From 2016–2019, he worked at EPFL-LMTS, Neuchâtel, Switzerland as a post-doctoral scientist on flexible, stretchable, and printing electronics, along with functional materials for energy harvesting, sensing and actuation. Currently, he is working as a post-doctoral scientist at Mechanical Engineering Department, Technical University of Denmark. His present research interests include micro- and nano-scale 3D printing for implantable sensor and actuator.

Martin Lubej received his M. Sc. and Ph. D. degree in Chemical Engineering from University of Ljubljana, Slovenia in 2014. In the year of 2018, he worked as a post-doctoral researcher at EPFL-LMTS, Neuchatel, Switzerland in the field of mathematical modeling and simulation of MEMS. He is currently employed as a computational fluid dynamics (CFD) expert in drug development at Novartis AG, Switzerland.

Danick Briand received his B. Eng. degree and M. A. Sc. degree in engineering physics from École Polytechnique in Montréal, Canada, in collaboration with the Institut National Polytechnique de Grenoble (INPG), France, in 1995 and 1997, respectively. He obtained his Ph. D. degree in Microtechnology from the University of Neuchâtel, Switzerland, in

2001. He is currently the team leader of the MEMS and Printed Microsystems group at the Soft Transducers Laboratory of EPFL. He has been author or co-author on more than 250 papers published in scientific journals and conference proceedings. His research interests include MEMS, digital manufacturing of smart sensing system, soft microsystems technologies, and green electronics.